Optimal model distributions in supervisory adaptive control

Ghosh, D.; Baldi, Simone

DOI
10.1049/iet-cta.2016.0679

Publication date
2017

Document Version
Accepted author manuscript

Published in
IET Control Theory and Applications

This is an Accepted Author Manuscript of an article published by Institution of Engineering and Technology (IET) in the journal IET Control Theory and Applications, available online: http://dx.doi.org/10.1049/iet-cta.2016.0679

Optimal Model Distributions in Supervisory Adaptive Control

Debarghya Ghosh [1] and Simone Baldi[2,*]

[1]Laboratoire Ampere, Ecole Centrale de Lyon, 69130 Ecully, France
[2]Delft Center for Systems and Control, Delft University of Technology, 2628 Delft, Netherlands

Abstract: Several classes of multi-model adaptive control schemes have been proposed in literature: instead of one single parameter-varying controller, in this adaptive methodology multiple fixed-parameter controllers for different operating regimes (i.e. different models) are utilized. Despite advances in multi-model adaptive control theory, the question of how the synthesis of the pairs model/controller will affect transient and steady-state performance is not completely addressed. In particular, it is not clear to which extent placing the pairs model/controller in a structurally optimal way will result in a relevant improvement of the properties of the switching algorithm. In this work we focus on a multi-model unfalsified adaptive supervisory switching control scheme, and we show how the minimization of a suitable structural criterion can lead to improved performance of the adaptive scheme. The peculiarity of the resulting structural optimality criterion is that the optimization is carried out so as to optimize the entire behavior of the adaptive algorithm, i.e. both the learning transient and the steady-state response. This is in contrast to alternative multi-model adaptive control schemes, where special structural optimization considers only the steady-state ideal response and neglects learning transients. A comparison with respect to model distributions achieved via two structural optimization criteria is made via a benchmark example.

1. Introduction

The emerging field of multi-model adaptive control has successfully mitigated classical adaptive control limitations by introducing logic-based adaptation [1]: instead of a single controller where the parameters vary and adapt with time multiple controllers, each one pertaining to a different operating regime (i.e. to a different model) and whose parameters are fixed, are used. The problem becomes the one of switching to the most appropriate controller in such a way to limit the poor transient that classical adaptive control might exhibit. The initial work on switching-based multi-model adaptive control led to two distinct families, namely the Unfalsified Adaptive Supervisory Switching Control [2, 3] and the Multi-model Adaptive Supervisory Switching Control schemes [4, 5, 6, 7]. The major downside of these multi-model adaptive control families is that none of them provides sufficient insight regarding where, within the uncertainty set covering the whole operating envelope, one should place the nominal models (and the corresponding candidate controllers) so as to achieve some optimal switching and steady-state performance.

Therefore, an existing open problem in the domain of multi-model adaptive control is the lack of insight regarding the placement locations of model/controller pairs within a given uncertainty set [8]. The best possible placement locations should be sought so that such performance is optimal with respect to a certain criterion. In this work, we demonstrate how the model/controller locations have a significant effect on the adaptive performance of the multi-model adaptive control scheme.

The term ‘adaptive performance’ encompasses factors like the length of learning transients, the swiftness with which the final controller is placed in the loop, and the amount of controller switches occurring before the final controller is turned on.

A novel multi-model adaptive control method was proposed recently, namely Multi-model Unfalsified Adaptive Supervisory Switching Control (MUASSC) [9, 10, 11, 12] that aims to tackle this issue by introducing an adaptive performance parameter that has a direct effect on the number of switches, and the maximum value achieved by the performance index. This parameter, that we refer to as the *structural optimality index* of the multi-model architecture, has been conceived such that it depends on both the synthesis methodology utilized to build the controller, and the distribution of the models within the given uncertainty.

Thus, the structural index can be related to the performance of the switching adaptive loop, and the research question arising naturally is whether, by minimizing this structural index, the corresponding model distribution would be the finest configuration of model/controller pairs that would lead to improved switching and steady-state performance. In this paper, we demonstrate how the model distribution that corresponds to the optimal structural index value indeed leads to superior switching and steady-state closed-loop performance as compared to suboptimal model distributions. The proposed structural optimization methodology is also compared to an alternative model distribution as suggested by the Robust Multi-Model Adaptive Control (RMMAC) architecture [13]. The peculiarity of the MUASSC structural optimization is that the optimization is carried out with respect to both the transients occurring during the learning period and the final steady-state system response. This is in contrast to the RMMAC structural index, which considers only the ideal steady-state response and neglects the transients during learning. We finally point out that multi-model adaptive control is closely related to fault tolerant control: fault tolerance is the property that enables a system to continue operating properly in the event of failures of some of its components (i.e. some change in the operating regime). Recent contributions in this field include [14, 15, 16, 17, 18]: to the best of the authors’ knowledge, also in fault tolerant control the problem of how to place the controllers (each controller corresponding to a different fault) in such a way to guarantee a desired reconfiguration performance has not been addressed. The study presented in this work can thus address fault tolerance issues like fast fault detection and reconfiguration via multiple models.

The paper is structured as follows: section 2 introduces the architecture of switching-based adaptive control, and presents the structural index linked to model distribution. Section 3 deals with how the structural parameter is optimized to arrive at the optimal model distribution for a given uncertainty set. Section 4 presents simulation results, followed by conclusions in section 5.

2. Supervisory adaptive control fundamentals with emphasis on MUASSC

The general structure utilized in the switching-based multi-model adaptive control consists of the four components illustrated in Fig. 1(a), namely: the plant, the multi-controller, the supervisor and the performance evaluator. In the sequel an overview of each component is provided.

2.1. The plant

The entity to be controlled is the plant $P \in \mathscr{P}$. The symbol $\mathscr{P}$ denotes the whole operating envelope of the plant: when the envelope is defined by parametric uncertainty, the envelope is

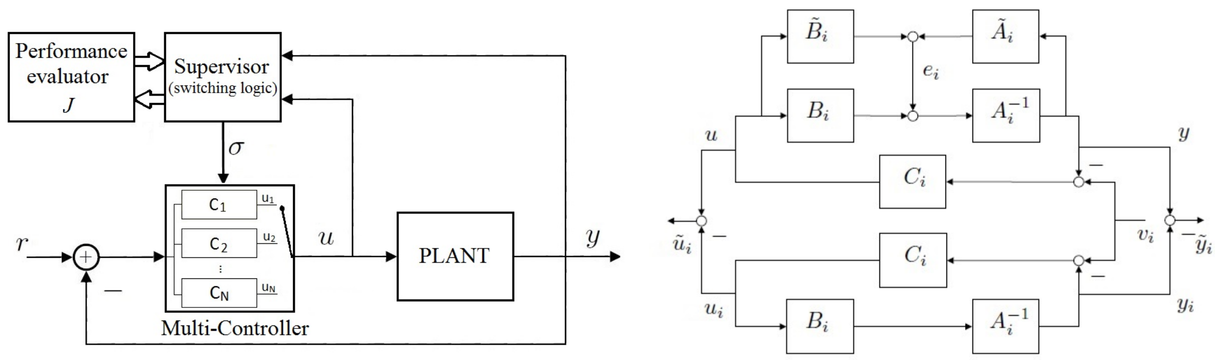

(a) Supervisory adaptive control architecture

(b) Mismatch plant (upper) and nominal model (lower) [9]

Fig. 1. *MUASSC basics*

represented by an uncertainty set Ω in which the uncertain parameters of the plant lie. A set of nominal models are used to represent some nominal operating conditions: these models are for simplicity represented with their transfer function in the delay operator d:

$$M_i(d) = B_i(d)/A_i(d), \quad i \in \overleftarrow{N} = \{1, 2, \dots, N\}$$

Having different nominal models corresponds to partitioning the whole uncertainty set Ω into N different subsets $\Omega = \bigcup_{i=1}^{N} \Omega_i$. Each nominal model $M_i(d)$ will be the representative of its own subset Ω_i. Intuitively, one can think that the partition has to be sufficiently dense in order to attain an approximation of the plant that is adequately tight. We will see that this is not always the case: in fact, a problem in multi-model adaptive control is the choice of the nominal models, i.e. finding a model distribution that optimizes some adaptation criterion.

2.2. The multi-controller

Corresponding to each nominal model $M_i(d)$, a candidate controller $C_i(d)$ is synthesized. Hence the multi-controller is a bank of these candidate controllers denoted with:

$$C_i(d) = S_i(d)/R_i(d), \quad i \in \overleftarrow{N}$$

Note that not only the model location, but also the controller will contribute to the stability and performance of the adaptive scheme, as it will be explained later.

Remark 1. *The presentation is carried out in the transfer function formalism: the numerical example in Section 3 will provide the guidelines in the equivalent state-space representation.*

2.3. Performance index evaluator

It has to be emphasized that the operating regime is not known in general. Only the input/output data u and y can be used for the selection of the most appropriate controller corresponding to the current (and uncertain) operating regime (e.g. think about a plant possibly subjected to faults). Toward this goal, the performance evaluator must generate a quantitative index used by the supervisor to produce σ, the controller index. The family of performance indices, one for each controller/model pair, is denoted as:

$$J_i(t): \quad i \in \overleftarrow{N}$$

Different performance indices have been formulated in literature [2, 3, 4, 6, 7]. In this work, the MUASSC performance index will be adopted. Referring to Fig. 1(b), we will denote a candidate loop with (P/C_i), i.e. the plant in feedback with a candidate controller C_i. We recall that the MUASSC performance index passes through the definitions of:

$$Q_i(d) \quad := \quad \frac{[-C_i(d) \quad 1]'}{(1 + M_i(d)\, C_i(d))\, A_i(d)} \tag{1}$$

and

$$\tilde{L}_i(d) := \left[\begin{array}{cc} \tilde{B}_i(d) & \tilde{A}_i(d) \end{array} \right] \tag{2}$$

where $\tilde{B}_i(d) = B(d) - B_i(d)$ and $\tilde{A}_i(d) = A(d) - A_i(d)$, where the true plant's transfer function is indicated with $P(d) = B(d)/A(d)$. From recorded input/output data z, the stability inference of a given candidate loop (P/C_i) is performed by estimating the magnitude $||Q_i\tilde{L}_i||_\infty$. Using the definition (1) and (2), it can be shown that the deviation between the actual control loop and a given pair controller/model (both driven by the virtual reference as defined in [2]), coincides with $||T_i||_\infty$, the generalized sensitivity matrix of the candidate loop (P/C_i)

$$\tilde{z}_i(t) = T_i(d) z_i(t) = (1 + P\, C_i)^{-1} \left[\begin{array}{cc} -\rho_i P C_i & \rho_i^{1/2} C_i \\ \rho_i^{1/2} P & -1 \end{array} \right] z_i(t) \tag{3}$$

where $\tilde{z}_i(t) := [\rho_i^{1/2}\tilde{u}_i(t) \quad \tilde{y}_i(t)]'$ and $z_i(t) := [\rho_i^{1/2} u_i(t) \quad y_i(t)]'$, $\rho_i > 0$. Hence, in the MUASSC scheme, a performance index that is often used is the estimate of $\|T_i\|_\infty$, which can be conveniently evaluated from plant data:

$$\Lambda_i(t) := \left\| \, \tilde{z}_i^t \, \right\|^2 / \left\| \, z_i^t \, \right\|^2, \quad J_i(t) := \max_t \Lambda_i(t) \tag{4}$$

where $\| \, \tilde{z}_i^t \, \|$ is the norm of the data sequence for all time intervals till time t: $\tilde{z}_i(0), \ldots, \tilde{z}_i(t)$.

Remark 2. *The interested reader can verify that the concepts the transfer functions (1) and (2) can be carried out in the equivalent state-space formulation. In particular, with reference to Fig. 1(b), one can see that (1) is the map between $[u\ y]'$ and e_i (closed-loop sensitivities) and (2) is the map between e_i and $[u\ y]'$ (deviation between the true and the nominal parameter values). Such maps can be found in the equivalent state-space representation via the state-space forms of P, M_i and C_i. A similar comment applies to the generalized sensitivity matrix T_i (which can be seen as the map between input/output disturbances and $[u\ y]'$.*

It is to be observed that, provided that $\mathscr{P}$ is a priori known and compact, for any candidate plant in $\mathscr{P}$, indices $i \in \overleftarrow{N}$ exists, that yield stable loops (P/C_i) such that $\left\| Q_i\, \tilde{L}_i \right\|_\infty < \beta < 1$, $\beta \in \mathbb{R}_+$. These indices that are stabilizing, are part of the set: $i \in S(P)$.

Such a model distribution for which the aforementioned property holds, is referred to as a β-*dense model distribution*. The value β arises from the solving the following in the all uncertainty set

$$\beta := \max_{P \in \mathscr{P}} \min_{i \in S(P)} \left\| Q_i\, \tilde{L}_i \right\|_\infty \tag{5}$$

Assuming that a β-*dense model distribution* exists, (P/C_i) possesses the β-*property* when $\left\| Q_i \, \tilde{L}_i \right\|_\infty < \beta$. The work [10] considers an class of dense model distributions, where β is allowed to be larger than 1. It can be seen from (5) that β depends on the closed-loop sensitivity in addition to the deviation between the true and the nominal parameter values. Consequently, the methodology of controller synthesis plays an important role in determining the value of parameter β, which from now on will be referred to as the *structural index* of the MUASSC scheme.

2.4. Supervisor (Switching logic)

The controller to be chosen is decided with the aid of a 'switching' logic that ultimately assigns a relevant controller index σ. Ideally, one would like to select the controller $C_\sigma(d)$, which corresponds to the smallest $J_\sigma(t)$: however, directly using this methodology leads to chattering in-between controllers, which can lead to instability. Consequently, this issue of chattering, a hysteresis switching logic [19] is widely used, as follows:

$$\sigma(t) = l(\sigma(t-1), J(t)), \quad \sigma(0) = i_0 \in \overleftarrow{N} \tag{6}$$

$$l(i, J(t)) = \begin{cases} i, & \text{if } J_i(t) < J_{\psi(J(t))}(t) + h \\ \psi(J(t)), & \text{otherwise} \end{cases} \tag{7}$$

Here $\psi(J)$ is the smallest integer $j \in \overleftarrow{N}$ where $J_j \leq J_i$, $\forall i \in \overleftarrow{N}$, and h, christened the *hysteresis constant*, is typically a small positive constant.

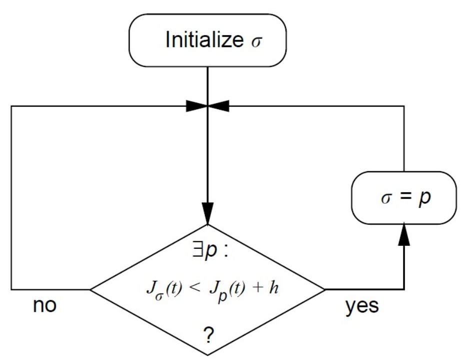

Fig. 2. *Hysteresis switching logic*

Remark 3. *The added advantage of introducing the hysteresis logic is that a change in the controller index occurs only when the 'more suitable' controller has a performance improvement of at least h [19] over the currently switched on controller. If such is not the case, and the improvement in J is inferior to h, the switching is avoided as the improvement is not good enough. This is shown schematically in Fig. 2. The algorithm of the switching logic represented in Fig. 2 is independent from the controller design.*

2.5. MUASSC stability and performance Theorem

If (4) is chosen as the MUASSC performance index, in combination with the switching logic (6), (7), then the following results, as stated in [9] are valid.

Theorem 1. Provided that at least one of the candidate controllers can stabilize the real plant P, for any initial condition and reference r, the switching stops in finite time, and the resulting MUASSC system $(P/C_{\sigma(\cdot)})$ is r-stable in the sense of [2]. Furthermore, if $\mathscr{P}$ is compact, under a β-dense model distribution $0 < \beta < 1$, then:

1. The total number of switches N_σ is upper-bounded by:
$$N_\sigma \leq N \left\lceil \frac{\beta^2}{h\,(1-\beta)^2} \right\rceil \tag{8}$$

2. The occurring condition $\forall\, \bar{s} \in S^c(P)$,
$$\Lambda_{\bar{s}}(t) \geq \frac{\beta^2}{(1-\beta)^2} \tag{9}$$
effectively guarantees that after time t, no controller that is potentially destabilizing will be switched-on;

3. Similarly, the occurring condition, $\forall\, \bar{s} \in S^c(P)$,
$$\Lambda_{\bar{s}}(t) \geq \frac{\beta^2}{(1-\beta)^2} + h \tag{10}$$
guarantees that any index active after time t will be associated to a stabilizing candidate controller.

4. When the condition $h \geq \beta^2/(1-\beta)^2$ is satisfied, each controller candidate will be placed in the loop only once, and if any controller that is stabilizing and possesses the previously introduced β-property, when placed in the feedback loop, cannot be turned off henceforth.

Meaning of theorem 1: The interpretation of Theorem 1 is now given. The theorem shows how lowering β can be advantageous towards improving the transient switching performance of the scheme. Relation (8) makes it clear that a lower β leads to reduced number of switches N_σ. Moreover, greater the N, the lower the value of β. Relations (9) and (10) can be more easily satisfied for smaller β: hence, the lower the β, the smaller the chances of a destabilizing controller being switched on. In addition to this, a lower β implies a smaller steady-state performance (in terms of the generalized sensitivity matrix in (3)). Finally, it is evident from the fourth point that a lower β mitigates the possibility of a wrong unwanted controller being switched on once the best controller is already in the loop. To summarize, Theorem 1 suggests that by lowering β, the performance of MUASSC (transient and steady state) should improve. The research question arising naturally is whether, by minimizing the structural index β, the corresponding model distribution is the finest configuration of model/controller pairs that would lead to the best possible switching and steady state performance. This hypothesis will be verified via a numerical benchmark example.

3. Benchmark example for comparison

In order to evaluate how the adaptive performance will change by changing the model distribution, we will adopt the classical two carts benchmark example, which is widely used to model suspension systems, smart structures, flexible space structures, etc. [20, 21, 22, 23]. The benchmark, shown in Fig. 3, consists of two carts, each one weighing $1Kg$ ($m_1 = m_2 = m = 1Kg$). The carts are interconnected via a spring of stiffness γ, which in-turn is the uncertain parameter and may vary between $\Gamma = [0.25, 1.5]N/m$, a prefixed known interval [9]. The system input is the force applied to the first cart and the output to be controlled is the second cart's position x_2. The state-space description of the bechmark with $m = 1Kg$ substituted is given by:

$$\dot{x} = (A_0 + \gamma A_1)x(t) + G_u u(t) \tag{11}$$
$$y(t) = \begin{bmatrix} 0 & 0 & 0 & 1 \end{bmatrix} x(t), \quad \text{with :}$$

$$A_0 = \begin{bmatrix} 0 & 1 & 0 & 0 \\ 0 & 0 & 0 & 0 \\ 0 & 0 & 0 & 1 \\ 0 & 0 & 0 & 0 \end{bmatrix}, \quad A_1 = \begin{bmatrix} 0 & 0 & 0 & 0 \\ -1 & 0 & 1 & 0 \\ 0 & 0 & 0 & 1 \\ 1 & 0 & -1 & 0 \end{bmatrix}, \quad G_u = \begin{bmatrix} 0 \\ 0 \\ 0 \\ 1 \end{bmatrix} \tag{12}$$

which in discrete-time, with sampling time T_s, results in the transfer function:

$$x_2 = \frac{\gamma T_s^4 d}{(d-1)^2[d^2 + (2\gamma T_s^2 - 2)d + 1]} \tag{13}$$

The following points are to be emphasized: first, no single (linear) controller can cope with the entire uncertainty set. So, to control the plant, a multi-controller has to be adopted. Second, due to the presence of integrators and a pair of purely imaginary poles, no PID controller can stabilize the plant (at least not in a robust way). Third, being based on a generalized sensitivity matrix, the MUASSC structural index is well posed only for linear controllers, which prevents from testing nonlinear control strategies like feedback linearization, sliding mode, etc. For theses reasons, the candidate controllers are designed based on H_∞ and LQ mixed sensitivity criterion [24] as follows:

$$H_\infty : \quad C_\gamma(s) = \arg \min_{\|r\|^2 \le 1} \frac{\|\tilde{r} - y\|^2 + \|u\|^2}{\|\tilde{r}\|^2} \tag{14}$$

$$\text{LQ} : \quad C_\gamma(s) = \arg \min_{\|r\|^2 \le 1} \|\tilde{r} - y\|^2 + \|u\|^2 \tag{15}$$

where $\tilde{r} = V(s)r$, and $V(s) = (s+2)^2(s^2 + \sqrt{2}s + 1)$ is a strictly Hurwitz polynomial to ensure pole placement [24]. The resulting controllers are discretized with sampling time $T_s = 0.1s$. The controllers are shown in Table 1 for a family of 3 and 5 candidate controllers. These controllers and the uncertainty set $\Gamma = [0.25, 1.5]N/m$ will be used for the calculation of the structural indices.

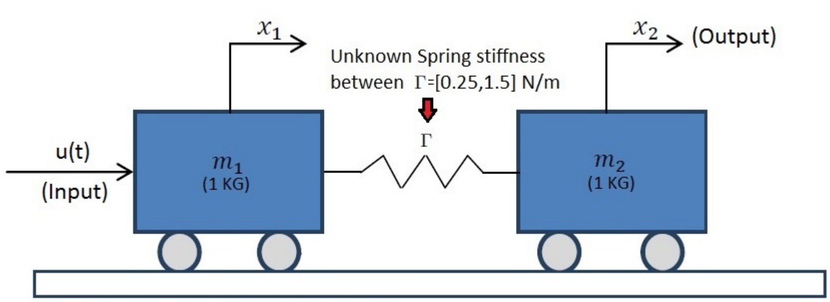

Fig. 3. *Two carts benchmark*

3.1. Optimization of the structural index β

The formulation of β in (5) sheds light on the fact that β depends on the deviation between the true plant and model parameters and hence the position of the models effects its value. In addition to this, β also depends on the closed-loop sensitivity and hence affected by the methodology used to synthesize the controller. For simplicity, it is assumed that all controllers are synthesized using the mixed sensitivity criterion [24]. This leads to a simplified optimization problem wherein the design variables of the problem can be restricted to the model/controller locations alone.

With reference to (5), one can observe that in the synthesis of β, max and min operators are used. Please refer to Fig. 4(a) and 5(a), which show how $\left\|Q_i\,\tilde{L}_i\right\|_\infty$ changes across the uncertainty, with 3 and 5 candidate controllers. The presence of such max and min operators lead to discontinuities in function values and hence smooth optimization algorithms would fail. In addition, the cost function is nonlinear in nature containing multiple minimas. Hence conventional off-the-shelf convex methodologies would fail to attain the global minimum. One therefore needs to use non-smooth, nonlinear optimization methodologies [25, 26] for possibly suited optimization techniques. A structural optimization algorithm has been proposed in [27] that takes advantage of a structure inherent to this specific minimization problem to efficiently arrive at the global minima: such an algorithm will be adopted in this work.

3.2. An alternative structural index

Among the different proposed approaches in multi-model adaptive control, the Robust Multi-Model Adaptive Control (RMMAC) is the only one where effort has been made towards attaining an optimal model distribution. In RMMAC the set of multi-models is places in such a way to guarantee an acceptable user defined degradation with respect to the mixed sensitivity achieved by an infinite set of local controllers covering the uncertainty set. For more details the reader is referred to [13]. Summarizing, the RMMAC technique accounts only for the steady-state mixed sensitivity performance, once the best controller is turned on. However there are no guarantees that the best controller will be placed in the loop. Moreover, no quantification on transient performance like total number of switches etc (e.g. Theorem 1 for MUASSC) is present in the RMMAC model distribution method. Thus, it is relevant to compare how model distributions that are structurally optimal with respect to the two different criteria will perform in transient and in steady-state conditions.

4. Simulation results

The β minimization technique introduced in [27] was utilized to optimize the MUASSC structural index. The simulations were carried out for two cases: 3 and 5 candidate controllers build up the multi-controller to tackle the uncertainty. All the model/controller pairs, before and after optimization, both the H_∞ and LQ synthesis, can be found in Tables 1 and 2.

3 candidate controllers: For the 3 controller case, the models are placed suboptimally at $[0.3, 0.5, 1.0]N/m$, corresponding to $\beta = 3.00$ for H_∞ synthesis and $\beta = 4.21$ for LQ synthesis. The minimization procedure places the models at $[0.3395, 0.62, 1.17]N/m$, corresponding to $\beta = 1.90$ for H_∞ synthesis, and $[0.3366, 0.6064, 1.227]N/m$, corresponding to $\beta = 2.54$ for LQ synthesis.

5 candidate controllers: For the 5 controller case, the models are placed as suggested by

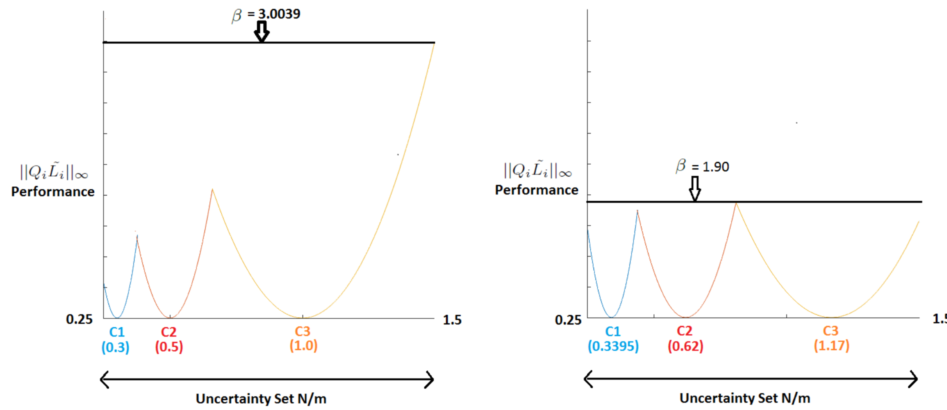

(a) Suboptimal model distribution (b) Optimal model distribution

Fig. 4. *H_∞ synthesis, 3 controllers case: structural index β*

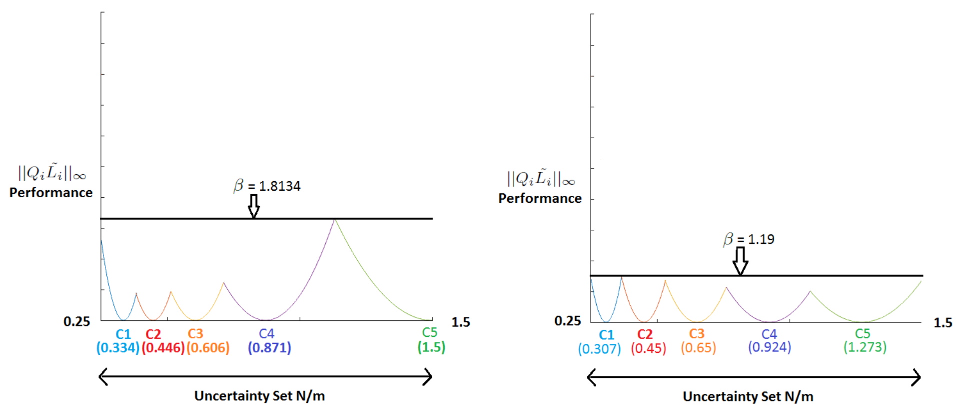

(a) Suboptimal model distribution (b) Optimal model distribution

Fig. 5. *H_∞ synthesis, 5 controllers case: structural index β*

the RMMAC scheme at $[0.334, 0.446, 0.606, 0.871, 1.50]N/m$, corresponding to $\beta = 1.81$ for H_∞ synthesis and $\beta = 2.46$ for LQ synthesis. The minimization procedure places the models at $[0.307, 0.45, 0.65, 0.924, 1.273]N/m$, corresponding to $\beta = 1.19$ for H_∞ synthesis, and $[0.334, , 0.229, 0.6717, 1.0484, 1.4683]N/m$, corresponding to $\beta = 1.85$ for LQ synthesis.

Due to the fact that the H_∞ synthesis culminated in a lower β for both the 3 and 5 controller cases, in the following we restrict the performance evaluation comparisons to the mixed sensitivity case alone. Figs. 4 and 5 show $\min_{i \in S(P)} \left\| Q_i \, \tilde{L}_i \right\|_\infty$ over the entire uncertainty set for 3 and 5 controllers, respectively, for both suboptimal and optimal model distribution. It is evident from Figs. 4 and 5 that by optimizing the locations of models one can achieve lower values of β.

Simulations are to be performed with the MUASSC scheme to prove the improvement in switching transient and steady-state performance before and after minimization of β. Different criteria are used to measure the performances:

- Criteria for switching transient performance
  - Final switching time
  - Number of switches before final switching time

Table 1. *Model/controller pairs: 3 candidate controllers*

Initial model/controller pairs	β	Final model/controller pairs	β
$[0.3; 0.5; 1.0] N/m$ MUASSC original, H_∞ synthesis $C_1 = \frac{43.43-129d+127.8d^2-42.3d^3}{1-2.388d+1.925d^2-0.5205d^3}$ $C_2 = \frac{26.5-79.04d+78.77d^2-26.23d^3}{1-2.372d+1.902d^2-0.5119d^3}$ $C_3 = \frac{13.28-40.38d+41.13d^2-14.02d^3}{1-2.322d+1.83d^2-0.4848d^3}$	3.00	$[0.3395; 0.62; 1.17] N/m$ MUASSC optimal, H_∞ synthesis $C_1 = \frac{38.65-114.9d+114d^2-37.75d^3}{1-2.384d+1.92d^2-0.5187d^3}$ $C_2 = \frac{21.06-63.02d+63.06d^2-21.1d^3}{1-2.362d+1.888d^2-0.5065d^3}$ $C_3 = \frac{11.43-35.28d+36.48d^2-12.63d^3}{1-2.286d+1.778d^2-0.4656d^3}$	1.90
$[0.3; 0.5; 1.0] N/m$ MUASSC original, LQ synthesis $C_1 = \frac{43.23-129.2d+126.9d^2-42.12d^3}{1-2.376d+1.921d^2-0.5202d^3}$ $C_2 = \frac{26.42-79.092d+78.15d^2-26.12d^3}{1-2.366d+1.907d^2-0.5136d^3}$ $C_3 = \frac{7.456-29.2d+42.98d^2-28.18d^3+6.938d^4}{1-3.339d+4.198d^2-2.354d^3+0.4961d^4}$	4.20	$[0.3395; 0.62; 1.17] N/m$ MUASSC optimal, LQ synthesis $C_1 = \frac{38.97-115.8d+114.9d^2-38.05d^3}{1-2.385d+1.921d^2-0.5189d^3}$ $C_2 = \frac{21.66-85.38d+126.4d^2-83.3d^3+20.61d^4}{1-3.33d+4.174d^2-2.334d^3+0.4904d^4}$ $C_3 = \frac{-2.133+8.872d-13.88d^2+9.692d^3-2.551d^4}{1-3.342d+4.207d^2-2.361d^3+0.4983d^4}$	2.59

  - Maximum input/output peak

- Criteria for steady state performance

  - Final controller-plant mixed sensitivity peaks

Remark 4. *It is important to underline that all these criteria are evaluated over the entire uncertainty set, and averaged over different controllers initially placed in the loop. This means that the uncertainty set* $[0.25, 1.5]N/m$ *has been divided into 250 discrete values and for every discrete point, simulations with different initial controllers are performed.*

4.1. Three controller comparisons: original vs optimal MUASSC structural index

Final switching time: The reader is directed towards Fig. 6(a), which shows the average highest switching time for both model distributions. As any one of the three controllers can be placed in the loop initially, Fig. 6(a) is the average of the final switching time. The results from Fig. 6(a) suggest that the highest switching time in the optimal case ($\beta = 1.9$) has been reduced to 944 seconds as compared to a previous highest switching time of 1056 seconds with a $\beta = 3.009$: consequently one can interpret this as an improved transient performance.

Number of switches: Table 3 shows the total number of switches occurring before the final controller is placed in the loop. It is observed that the overall total number of switches reduces from 3 switches in the suboptimal model distribution, to 2 in the optimal one. According to the first part of Theorem 1, if β is reduced, then one may expect the *upper bound* on the number of switches to go down. Our simulations indicate that also the *actual number of switches* goes down, which is not an obvious result. These comparisons prove that the model distribution corresponding to the optimal β does indeed yield superior switching performance when compared with the suboptimal one.

Mixed sensitivity peak: Fig. 6(b) shows the mixed sensitivity peak (i.e steady-state performance) resulting from the combination of the final controller and plant. The results of the mixed

Table 2. *Model/controller pairs: 5 candidate controllers*

Initial placement	β	Final Placement	β
$[0.334; 0.446; 0.606; 0.871; 1.50]N/m$ RMMAC, H_∞ synthesis $C_1 = \frac{39.25-116.6d+115.7d^2-38.33d^3}{1-2.385d+1.921d^2-0.5189d^3}$ $C_2 = \frac{29.68-88.4d+87.96d^2-29.24d^3}{1-2.376d+1.908d^2-0.5141d^3}$ $C_3 = \frac{21.85-65.35d+65.35d^2-21.84d^3}{1-2.364d+1.891d^2-0.5075d^3}$ $C_4 = \frac{15.17-45.82d+46.32d^2-15.67d^3}{1-2.34d+1.855d^2-0.4941d^3}$ $C_5 = \frac{9.043-29.66d-32.47d^2+11.84d^3}{1-2.153d+1.588d^2-0.3957d^3}$	1.81	$[0.307; 0.45; 0.65; 0.924; 1.273]N/m$ MUASSC optimal, H_∞ synthesis $C_1 = \frac{42.5-126.2d+125.1d^2-41.42d^3}{1-2.387d+1.924d^2-0.5202d^3}$ $C_2 = \frac{29.42-87.64d+87.21d^2-28.99d^3}{1-2.376d+1.9078d^2-0.5139d^3}$ $C_3 = \frac{20.36-60.96d+61.05d^2-20.44d^3}{1-2.361d+1.886d^2-0.5056d^3}$ $C_4 = \frac{14.32-43.36d+43.96d^2-14.91d^3}{1-2.333d+1.846d^2-0.4906d^3}$ $C_5 = \frac{10.68-33.35d-34.89d^2-12.21d^3}{1-2.259d+1.738d^2-0.451d^3}$	1.19
$[0.334; 0.446; 0.606; 0.871; 1.50]N/m$ RMMAC, LQ synthesis $C_1 = \frac{34.93-135.3d+196.7d^2-127.1d^3+30.79d^4}{1-3.31d+4.128d^2-2.297d^3+0.4806d^4}$ $C_2 = \frac{23.99-93.38d+136.4d^2-88.61d^3+21.6d^4}{1-3.333d+4.185d^2-2.343d^3+0.493d^4}$ $C_3 = \frac{21.19-83.26d+122.9d^2-80.74d^3+19.92d^4}{1-3.348d+4.22d^2-2.372d^3+0.5009d^4}$ $C_4 = \frac{9.74-38.14d+56.12d^2-36.77d^3+9.052d^4}{1-3.351d+4.228d^2-2.378d^3+0.5026d^4}$ $C_5 = \frac{-1.807+7.341d-11.22d^2+7.665d^3-1.977d^4}{1-3.36d+4.25d^2-2.396d^3+0.5075d^4}$	2.46	$[0.334; 0.4229; 0.6717; 1.0484; 1.4683]N/m$ MUASSC optimal, LQ synthesis $C_1 = \frac{34.9-135.3d+196.7d^2-127.1d^3+30.79d^4}{1-3.31d+4.128d^2-2.297d^3+0.4806d^4}$ $C_2 = \frac{26.3-102.4d+149.7d^2-97.33d^3+23.74d^4}{1-3.332d+4.182d^2-2.341d^3+0.4925d^4}$ $C_3 = \frac{13.31-51.92d+76.05d^2-49.57d^3+12.13d^4}{1-3.345d+4.213d^2-2.366d^3+0.4994d^4}$ $C_4 = \frac{-2.944+12.21d-19.04d^2+13.24d^3-3.467d^4}{1-3.351d+4.23d^2-2.379d^3+0.5031d^4}$ $C_5 = \frac{-4.417+17.73d-26.8d^2+18.1d^3-4.611^4}{1-3.359d+4.248d^2-2.394d^3+0.5072d^4}$	1.85

Table 3. *3 controllers case: transient and steady-state performance criteria*

Locations of Controllers	Original MUASSC	Optimal MUASSC	Reduction %
Highest switching time	1080 s	930 s	13.9%
Highest number of switches (Overall, for all initial conditions)	3 switches	2 switches	33.3%
P/C_i Mixed Sensitivity peak	70 % of uncertain set experienced a lower peak value		

sensitivity showed that almost 70% of the set experienced a lower mixed sensitivity peak, around 28% faced degradation while the rest 2% remained almost the same. Note that, in Fig. 6(b), only the portions of uncertainty where the final controller is active have been plotted. The discontinuities in Fig. 6(b) indicate the change in the final controller between one spring stiffness and another. Hence as a collective set, the steady-state performance is improved by the optimal model distribution.

4.2. Five controller comparisons: MUASSC vs RMMAC structural index

Final switching time: In these simulations the averaging of the final switching time is done out of five possible initial controllers. Fig. 7(a) and Table 4 indicate that the highest switching time for MUASSC model distribution is limited to 380 seconds as compared to 540 seconds in the RMMAC model distribution.

Number of switches: Fig. 7 shows that the total number of switches reduced from 2 in the RMMAC model distribution to 1 in the MUASSC optimal model distribution. Consequently, the

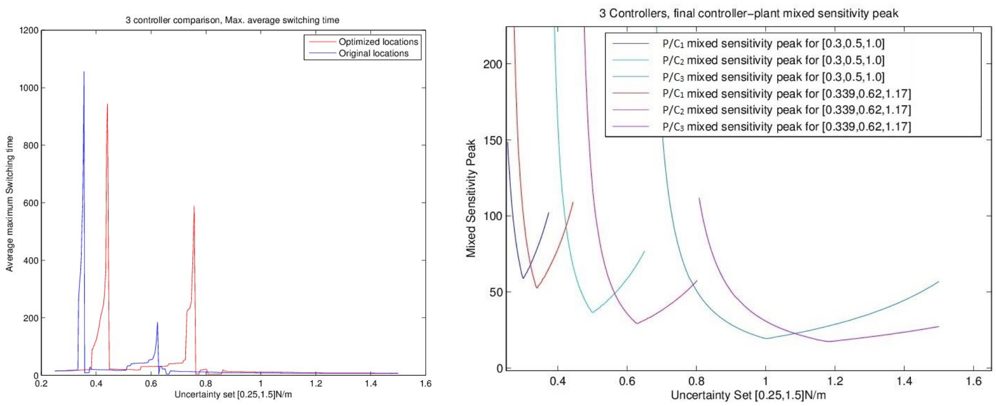

(a) Highest switching time

(b) Mixed sensitivity peaks

Fig. 6. *H_∞ synthesis, 3 controllers case*

Table 4. *5 controllers case: transient and steady-state performance criteria*

Locations of Controllers	RMMAC	Optimal MUASSC	% Reduction
Highest switching time	540 s	380 s	29.6%
Highest number of switches (Overall, for all initial conditions)	2 switches	1 switch	50%
P/C_i Mixed Sensitivity peak	80 % of uncertain set experienced a lower peak value		

reducing of β led to better transient MUASSC performance for both $N = 3$ and $N = 5$.

Mixed sensitivity peak: The mixed sensitivity peak in Fig. 7(b) shows clearly that for the uncertainty set as a whole, the peak is reduced for almost 80% of the set, with a 20% performance degradation elsewhere. Again this suggests that irrespective of N, optimizing β leads not only to superior transient performance but also improved steady-state performance. The results of the five controller case are concisely presented in Table 4.

5. Conclusions

This work demonstrated how the minimization of a suitable structurally optimal criterion can lead to improved performance of the MUASSC scheme. The structural index depends on the location of the model/controller pairs, also referred to as model distribution. It was the hypothesis that the model distribution the would correspond to the lowest possible structural index could yield optimal transient and steady state performance. A numerical benchmark example clearly shows that a lower structural index can decrease the 'number of switches' before the final controller is inserted. A reduction of the 'final switching time' is also observed. In addition, the theoretical mixed sensitivity peak comparisons also indicated a better steady state performance for a greater part of the set with the final controller being switched on.

In retrospect, when comparing MUASSC with RMMAC, the structural index of MUASSC and RMMAC, the structural index in MUASSC guarantees a desired transient performance, while in the RMMAC case no such guarantee can be provided. Future work will involve development of fast and efficient non smooth non linear algorithms that can speed up the convergence of this structural optimization problem. Furthermore, the definition of the structural index is limited to

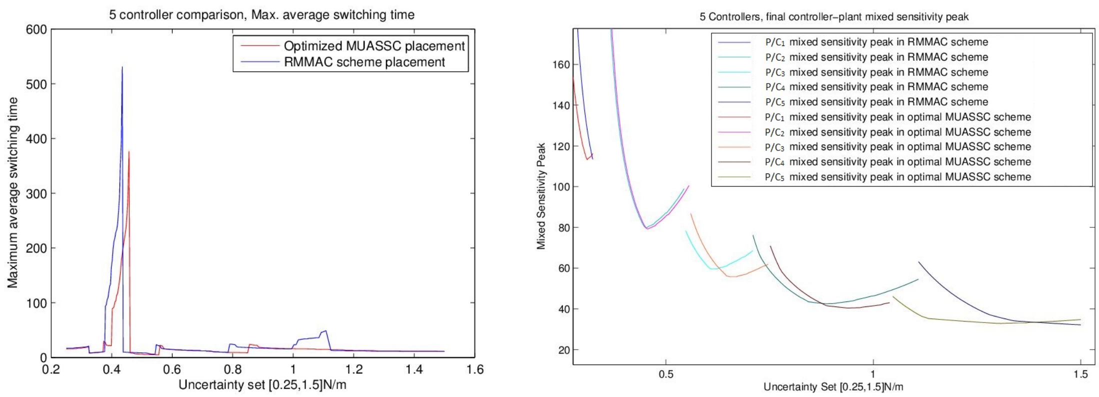

(a) Highest switching time

(b) Mixed sensitivity peaks

Fig. 7. *H_∞ synthesis, 5 controllers case*

linear systems and linear controllers. Extensions to nonlinear cases is an open problem and might be addressed in the future.

6. References

[1] Landau, I.D., Lozano, R., M'Saad, M., Karimi, A.: '*Adaptive Control - Algorithms, Analysis and Applications*', Springer, 2011

[2] Safonov, M. G., Tsao, T.C.: 'The Unfalsified Control Concept and Learning', *IEEE Transactions on Automatic Control*, 1997, **42**, pp. 843 - 847

[3] Stefanovic, M., Safonov, M. G.: 'Safe Adaptive Switching Control: Stability and Convergence', *IEEE Transactions on Automatic Control*, 2008, **53**, pp. 2012 - 2021

[4] Narendra, K. S., Balakrishnan, J.: 'Adaptive control using multiple models', *IEEE Transactions on Automatic Control*, 1994, **42**, pp. 171 - 187

[5] Hespanha, J., Liberzon, D., Morse, A. S., Anderson, B., Brinsmead T. S., De Bruyne, F.: 'Multiple model adaptive control. Part 2: switching', *International Journal of Robust and Nonlinear Control*, 2001, **11**, pp. 479 - 496

[6] Angeli, D., Mosca, E.: 'Lyapunov-Based Switching Supervisory Control of Nonlinear Uncertain Systems', *IEEE Transactions on Automatic Control*, 2002, **47**, pp. 500 - 505

[7] Baldi, S., Ioannou, P. A., Kosmatopoulos, E. B.: 'Adaptive mixing control with multiple estimators', *International Journal of Adaptive Control and Signal Processing*, 2012, **26**, pp. 800 - 820

[8] Anderson, B., Brinsmead T. S., De Bruyne, F., Hespanha, J., Liberzon, D., Morse, A. S.: 'Multiple model adaptive control. Part 1: Finite controller coverings', *International Journal of Robust and Nonlinear Control*, 2000, **10**, pp. 909 - 929

[9] Baldi, S., Battistelli, G., Mosca, E., Tesi, P.: 'Multi-Model Unfalsified Adaptive Switching Supervisory Control', *Automatica*, 2013, **46**, pp. 249 - 259

[10] Baldi, S., Battistelli, G., Mosca, E., Tesi, P.: 'Multi-model unfalsified adaptive switching control: Test functionals for stability and performance', *International Journal of Adaptive Control and Signal Processing*, 2013, **25**, pp. 593 - 612

[11] Baldi, S., Battistelli, G., Mosca, E., Tesi, P.: 'Multi-model unfalsified switching control of uncertain multivariable systems', *International Journal of Adaptive Control and Signal Processing*, 2013, **26**, pp. 705 - 722

[12] Baldi, S., Ioannou, P., Mosca, E.: 'Evaluation of identifier based and & non-identifier based adaptive supervisory & control using a benchmark example', *2010 4th International Symposium on Communications, Control and Signal Processing (ISCCSP)*, 2010, pp. 1-6

[13] Fekri, S., Athans, M., Pascoal, A.: 'Issues, progress and new results in robust adaptive control', *International Journal of Adaptive Control and Signal Processing*, 2006, **20**, pp. 519 - 579

[14] Li, Y., Yang, G.-H.: 'Robust fuzzy adaptive fault-tolerant control for a class of nonlinear systems with mismatched uncertainties and actuator faults', *Nonlinear Dynamics*, 2015, **81**, pp. 395 - 409

[15] Li, Y., Yang, G.-H.: 'Fuzzy Adaptive Output Feedback Fault-Tolerant Tracking Control of a Class of Uncertain Nonlinear Systems With Nonaffine Nonlinear Faults', *IEEE Transactions on Fuzzy Systems*, 2013, **24**, pp. 223 - 234

[16] Li, Y., Yang, G.-H.: 'Adaptive Fuzzy Decentralized Control for a Class of Large-Scale Nonlinear Systems With Actuator Faults and Unknown Dead Zones', *IEEE Transactions on Systems, Man, and Cybernetics: Systems*, 2016, **99**, pp. 1 - 12

[17] Yang, G. , Ye, D.: 'Reliable Control H_∞ of Linear Systems With Adaptive Mechanism', *IEEE Transactions on Automatic Control*, 2010, **55**, pp. 242 - 247

[18] Li, Y.-X., Yang, G.-H.: 'Robust Adaptive Fault-Tolerant Control for a Class of Uncertain Nonlinear Time Delay Systems', *IEEE Transactions on Systems, Man, and Cybernetics: Systems*, 2017, to appear

[19] Hespanha, J. P., Liberzon, D., Morse, A. S.: 'Hysteresis-based switching algorithms for supervisory control of uncertain systems', *Automatica*, 2003, **39**, pp. 263 - 272

[20] Hingane, A., Sawant, S. H., Chavan, S. P., Shah, A. P.: 'Analysis of Semi active Suspension System with Bingham Model Subjected to Random Road Excitation Using MATLAB/Simulink', *IOSR Journal of Mechanical and Civil Engineering*, 2006, **03**, pp. 01 - 06

[21] Chikhale, S. J., Deshmukh, S. P.: 'Comparative Analysis Of Vehicle Suspension System in Matlab-SIMULINK and MSc- ADAMS with the help of Quarter Car Model', *International Journal of Innovative Research in Science, Engineering and Technology*, 2013, **02**, pp. 4074 - 4081

[22] Dowds, P., O'Dwyer, A.: 'Modelling and control of a suspension system for vehicle applications', *Proceedings of the 4th Wismarer Automatisierungs Symposium, Wismar, Germany, September 22-23*, 2005

[23] Lee J., J.: *'H_∞ control of Flexible Structures'*, MSc dissertation, University of Hawaii at Manoa, 1997

[24] Kwakernaak, H.: 'Robust Control and H_∞ Optimization Tutorial Paper', *Automatica*, 1993, **29**, pp. 255 - 273

[25] Hestenes, M. R.: 'Multiplier and gradient methods', *Journal of Optimization Theory and Applications*, 1969, **4**, pp. 303 - 320

[26] Mifin, R.: 'A modication and an extension of Lemarechal's algorithm for nonsmooth minimization', *Nondifferential and variational techniques in optimization (Sorensen D. C., Wets, R. J. B., eds.)*, 1982, **17**, pp. 77 - 90

[27] Ghosh, D., Baldi, S.: 'Algorithms for Optimal Model Distributions in Adaptive Switching Control Schemes.' *Machines*, 2016, **4**, pp. 7